

Four loop $\overline{\text{MS}}$ mass anomalous dimension in the Gross-Neveu model

J.A. Gracey,
Theoretical Physics Division,
Department of Mathematical Sciences,
University of Liverpool,
P.O. Box 147,
Liverpool,
L69 3BX,
United Kingdom.

Abstract. We compute the four loop term of the mass anomalous dimension in the two dimensional Gross-Neveu model in the $\overline{\text{MS}}$ scheme. The absence of multiplicative renormalizability which results when using dimensional regularization means that the effect of the evanescent operator, which first appears at three loops in the 4-point Green's function, has to be properly treated in the construction of the renormalization group function. We repeat the calculation of the three loop $\overline{\text{MS}}$ β -function and construct the β -function of the evanescent operator coupling which corrects earlier computations.

1 Introduction.

The Gross-Neveu model is a two dimensional asymptotically free renormalizable quantum field theory whose basic interaction is a simple quartic fermion self-interaction, [1]. It has been widely studied since its introduction in [1], as it has many interesting properties which are readily accessible given the space-time dimension the model is defined in. For instance, unlike the same interaction in four dimensions it is renormalizable in two dimensions and the generation of mass dynamically has been observed and studied in the large N expansion, [1]. Moreover, one property of interest is that it possesses an S -matrix whose *exact* form is known, [2, 3], whence the mass gap is known exactly, [4], in terms of the basic mass scale of the theory, $\Lambda_{\overline{\text{MS}}}$. Aside from these features the model itself underpins several problems in condensed matter physics. For instance, in the replica limit it is equivalent at the critical point to the two dimensional random bond Ising model. (See, for example, the review [5].) Necessary to study the fixed point properties for such physical problems is knowledge of the renormalization group functions in some renormalization scheme, such as $\overline{\text{MS}}$. These have been computed to three loops in $\overline{\text{MS}}$ over a period of years. In [1] the one loop β -function was computed demonstrating asymptotic freedom. This was extended to two loops in [6], whilst the three loop β -function appeared more or less simultaneously in [7] and [8]. Though the method of computation in both articles was significantly different. For instance, given the quartic nature of the sole interaction it can be rewritten in terms of an auxiliary field producing a trivalent interaction with the introduction of an auxiliary field. This was the version of the theory used in [8], as well as at two loops in [6], not only to deduce the β -function but also to study the effective potential of the auxiliary field at three loops. However, renormalization effects will generate a quartic interaction. So [8] had in effect to handle the intricate problem of renormalizing a version of the theory with two independent couplings. The three loop $\overline{\text{MS}}$ β -function of the original theory was eventually extracted when the effect of the newly generated interaction was properly accounted for in the renormalization group equations. By contrast, in [7] the purely quartic version of the theory was treated with a massive fermion. The agreement of both three loop results was a reassuring non-trivial check on the final expression. At four loops only the wave function renormalization has been computed in [9] and later verified in [10]. Although apparently one loop further than the β -function of [7, 8], or mass anomalous dimension, [11], the fermionic nature of the interaction means that the anomalous dimension begins at two loops since the one loop snail graph is zero in the wave function channel of the 2-point function. Thus in effect the four loop wave function is a computation on a par with the three loop mass anomalous dimension and β -function.

Given the range of problems which the Gross-Neveu model underlies, it is the purpose of this article to start the programme of completing our knowledge of the four loop structure by computing the mass anomalous dimension at this order in the $\overline{\text{MS}}$ scheme. This may appear to be the least important of the two outstanding quantities. However, as will become apparent from the calculation we will describe, the nature of the model is such that there are several difficult technical issues to be dealt with en route which do not arise in other four loop calculations in other important theories. Therefore, in one sense we are testing the viability of computing renormalization constants at four loops in an example in the Gross-Neveu model which contains a moderate number of Feynman diagrams rather than the 1000 plus graphs which will occur in the 4-point function renormalization *and* with a sensible investment of time. Moreover, the experience gained in such an exercise will be invaluable for any future such coupling constant renormalization. It will transpire that we will require properties of Feynman integrals in two space-time dimensions higher than the one we compute in, in order to determine the final renormalization group function. Whilst this may not be the unique way to determine this, it will suggest the importance of the structure of higher dimensional Feynman diagrams in

complementing practical lower dimensional calculations and potentially *equally* vice versa at high loop order. Our main tool of computation will be the use of dimensional regularization in $d = 2 - \epsilon$ dimensions where the relevant part of the 2-point function is written in terms of basic massive vacuum bubble graphs. Such a calculation could only be completed with the use of computer algebra and invaluable in this was the symbolic manipulation language FORM, [12]. At this level of loop order automatic Feynman diagram computation using computers is the only viable way of keeping a reliable account of the algebra within a reasonable time. Several other computer packages were also required.

As this is the first four loop calculation which involves *four* terms of the renormalization group functions, we will have to revisit and redo the earlier calculations using the same approach consistently as that which will be used here at four loops. For reasons which will become evident later this has entailed us carrying out the full renormalization of the 4-point function in the theory with a massive fermion, where the mass will act as a natural infrared regulator. In [7] and [8] these articles centred on the derivation of the three loop β -function itself, which unlike most field theories, is not the same as fully renormalizing the underlying n -point function. For the Gross-Neveu model this was first observed in [13, 14] with explicit three loop calculations for the full 4-point function given for a massless version of the theory discussed in the series of articles [15, 16, 17] and examined in [18] for the massive version. However, neither computation was in complete agreement as to the final structure of the 4-point function renormalization. Prior to considering any four loop mass anomalous dimension this discrepancy needs to be resolved in one way or another which is a secondary consideration for this article. Any four loop β -function computation would also require this resolution but constructing the mass anomalous dimension in a consistent way is an easier environment in which to *check* any final explanation.

The paper is organised as follows. We review the current understanding of the renormalization properties of the Gross-Neveu model in section 2. Given this we discuss the three loop vacuum bubble integrals needed for the full three loop renormalization in section three. There we resolve the discrepancy between [17] and [18] in the 4-point renormalization in section 4. Section 5 extends the discussion of the relevant vacuum bubble computations to four loops with the four loop mass anomalous finally being derived in section 6. Concluding remarks are given in section 7.

2 Preliminaries.

We turn now to the specific properties of the Gross-Neveu model. The bare two dimensional Lagrangian is, [1],

$$L = i\bar{\psi}_0^i \not{\partial} \psi_0^i - m_0 \bar{\psi}_0^i \psi_0^i + \frac{1}{2} g_0 (\bar{\psi}_0^i \psi_0^i)^2 \quad (2.1)$$

where the subscript $_0$ denotes a bare quantity and g is the coupling constant which is dimensionless in two dimensions. Unlike [7, 11] which used the symmetry group $O(N)$ we take the $SU(N)$ version of the theory so that the fermion field ψ^i is a complex Majorana fermion with the former property deriving from the fields taking values in the group $SU(N)$ with $1 \leq i \leq N$. An advantage of the choice of the group $SU(N)$ is that the Feynman rule of (2.1) involves two terms unlike the three of the $O(N)$ case. At four loops this reduces the number of terms needed to be substituted when the Feynman rules are implemented in FORM which speeds up the calculation. We choose to work with the massive version where m is the mass. This is primarily because we will need to redo the three loop renormalization of the coupling and the presence of a non-zero mass will ensure that any resulting divergences are purely ultraviolet and not deriving from spurious infrared infinities which could arise when external momenta are

nullified in the basic divergent 4-point Green's function. In two dimensions the theory (2.1) is renormalizable to all orders in the coupling constant and is asymptotically free. Specifically we note that the $\overline{\text{MS}}$ scheme renormalization group functions of the model, as they currently stand are, [1, 6, 7, 8, 9, 11, 17],

$$\begin{aligned}
\gamma(g) &= (2N-1)\frac{g^2}{8\pi^2} - (N-1)(2N-1)\frac{g^3}{16\pi^3} \\
&\quad + (4N^2 - 14N + 7)(2N-1)\frac{g^4}{128\pi^4} + O(g^5) \\
\gamma_m(g) &= -(2N-1)\frac{g}{2\pi} + (2N-1)\frac{g^2}{8\pi^2} + (4N-3)(2N-1)\frac{g^3}{32\pi^3} + O(g^4) \\
\beta(g) &= (d-2)g - (N-1)\frac{g^2}{\pi} + (N-1)\frac{g^3}{2\pi^2} + (N-1)(2N-7)\frac{g^4}{16\pi^4} \\
&\quad + O(g^5)
\end{aligned} \tag{2.2}$$

where $\gamma(g)$, $\gamma_m(g)$ and $\beta(g)$ are respectively the field and mass anomalous dimensions and the β -function. Their formal definitions will be discussed later. Although several terms were determined for the $O(N)$ version of the model, we have converted the previous computations to the $SU(N)$ model whence the free field case emerges when $N = \frac{1}{2}$ as indicated by the vanishing of $\gamma(g)$ and $\gamma_m(g)$ for this value.

In the computations deriving (2.2) the main strategy was to dimensionally regularize (2.1) in d -dimensions and determine the renormalization constants as poles in the deviation from two dimensions. Here we will take $d = 2 - \epsilon$ with ϵ being regarded as small. Whilst the correct renormalization group functions emerged at three loops, [8] overlooked a novel feature of the dimensionally regularized Lagrangian which was explicitly discussed in [15, 16] after the observation in [13, 14]. Basically (2.1) ceases being multiplicatively renormalizable in d -dimensions but crucially retains renormalizability. This is not a property solely restricted to the Gross-Neveu model but is a feature of any two dimensional model with a 4-fermi interaction such as the abelian and non-abelian Thirring models, [18]. At a certain loop order, which is different for different models, evanescent operators are generated through the renormalization which are non-trivial in d -dimensions but which are absent or evaporate in the limit to strictly two dimensions which corresponds to the lifting of the regularization. A comprehensive study of this problem was provided for general 4-fermi theories in [13, 14] and we recall those features which are relevant for our ultimate goal. The same problem in four dimensions has been considered in [19, 20]. Though there 4-fermi operators are of course non-renormalizable and treated in the context of effective field theories.

First, in d -dimensions the basis of γ -matrices based on the Clifford algebra

$$\{\gamma^\mu, \gamma^\nu\} = 2\eta^{\mu\nu} \tag{2.3}$$

has to be extended to the set of objects $\Gamma_{(n)}^{\mu_1 \dots \mu_n}$ for integer $n \geq 0$, [13, 14, 15, 16, 17], which is totally antisymmetric in the Lorentz indices and defined by

$$\Gamma_{(n)}^{\mu_1 \mu_2 \dots \mu_n} = \gamma^{[\mu_1} \gamma^{\mu_2} \dots \gamma^{\mu_n]} \tag{2.4}$$

where we use the convention that the square brackets include division by $n!$ when all possible permutations of the γ -strings are written explicitly. Then $\Gamma_{(n)}^{\mu_1 \dots \mu_n}$ form a complete closed basis for γ -matrices in d -dimensions where $\Gamma_{(0)}$ is the unit matrix. Hence one can immediately see that the most general multiplicatively renormalizable 4-fermi theory using dimensional regularization in d -dimensions is, [13, 14, 15, 16, 17],

$$L = i\bar{\psi}_0^i \not{\partial} \psi_0^i - m_0 \bar{\psi}_0^i \psi_0^i + \frac{1}{2} \sum_{n=0}^{\infty} g_{(n)0} \bar{\psi}_0^i \Gamma_{(n)}^{\mu_1 \dots \mu_n} \psi_0^i \bar{\psi}_0^j \Gamma_{(n)}{}_{\mu_1 \dots \mu_n} \psi_0^j \tag{2.5}$$

where there is an infinite number of (bare) couplings $g_{(n)0}$ with $g_{(0)} \equiv g$ identified as the original one of the Gross-Neveu model (2.1). Though the Gross-Neveu model strictly will correspond to the case where $g_{(1)} = g_{(2)} = 0$ as $\Gamma_{(1)}^\mu$ and $\Gamma_{(2)}^{\mu\nu}$ are not evanescent. Given (2.5), there are several points of view depending on the problem in hand. If (2.5) is the most general renormalizable theory in d -dimensions, then in principle for the Gross-Neveu model one must begin with (2.5) but omit $g_{(1)}$ and $g_{(2)}$. This will produce renormalization group functions dependent, in principle, on all evanescent couplings. The true renormalization group functions of the original theory would eventually emerge from this multiplicatively renormalizable theory by setting $g_{(n)} = 0$ for $n \geq 3$ at the end, [13, 14, 15, 16, 17]. Clearly this would involve a significant amount of calculation much of which would be redundant in the production of the final renormalization group functions. From a practical point of view there is a less laborious route to follow if one abandons the insistence on multiplicative renormalizability, [17, 18]. Then operators such as

$$\mathcal{O}_n = \frac{1}{2} \bar{\psi}^i \Gamma_{(n)}^{\mu_1 \dots \mu_n} \psi^i \bar{\psi}^i \Gamma_{(n)} \psi^i \quad (2.6)$$

for $n \geq 3$ will be generated with $g_{(0)} \equiv g$ dependent coefficients. The problem for this point of view then becomes one of how to extract the *true* two dimensional renormalization group functions. It turns out that a formalism was developed in [13, 14] and used in [18, 10] for this evanescent operator issue. In essence the true renormalization group functions are not strictly determined from what we term the naive renormalization constants. By these we mean those required to render 2 and 4-point functions finite. Instead these naive renormalization group functions need to be amended by the effect the evanescent operators have on the divergence structure in d -dimensions relative to two dimensions. In [13, 14] such a projection formula was introduced which involves projection functions, $\rho^{(k)}(g)$, $\rho_m^{(k)}(g)$ and $C^{(k)}(g)$, where the index k ranges over the evanescent range $k \geq 3$. These functions quantify the effect the evanescent operators have on the derivation of the renormalization group functions. The derivation of the projection formula is given in [14] and applied additionally in [18, 10]. We recall that it is

$$\begin{aligned} \int d^d x \mathcal{N}[\mathcal{O}_k] \Big|_{g_{(i)}=0, d=2} &= \int d^d x \left(\rho^{(k)}(g) \mathcal{N}[i\bar{\psi}\not{\partial}\psi - m\bar{\psi}\psi + 2g\mathcal{O}_0] \right. \\ &\quad \left. - \rho_m^{(k)}(g) \mathcal{N}[m\bar{\psi}\psi] + C^{(k)}(g) \mathcal{N}[\mathcal{O}_0] \right) \Big|_{g_{(i)}=0, d=2} \end{aligned} \quad (2.7)$$

where the normal ordering symbol, \mathcal{N} , is included, [13, 14, 21, 22]. The relation strictly only has meaning when inserted in a 2 or 4-point Green's function. In other words one inserts the evanescent operator of the left side of (2.7) in a Green's function and evaluates it using the naive renormalization constants to yield a finite expression. Equally one inserts the left side of (2.7) into the same Green's function to the same loop order and renders it finite. Then the coefficients of the perturbative expansion in the coupling constant g are chosen order by order to render the equation consistent at each loop order after one has set $d = 2$. This procedure is denoted by the restriction $\{g_{(i)} = 0, d = 2\}$ on both sides of (2.7). Once the explicit projection functions have been determined to the appropriate order, then the *true* renormalization group functions are given by, [13, 14],

$$\begin{aligned} \beta(g) &= \tilde{\beta}(g) + \sum_{k=3}^{\infty} C^{(k)}(g) \beta_k(g) \\ \gamma(g) &= \tilde{\gamma}(g) + \sum_{k=3}^{\infty} \rho^{(k)}(g) \beta_k(g) \\ \gamma_m(g) &= \tilde{\gamma}_m(g) + \sum_{k=3}^{\infty} \rho_m^{(k)}(g) \beta_k(g) \end{aligned} \quad (2.8)$$

where $\tilde{}$ denotes the *naive* renormalization group functions.

For the Gross-Neveu model the first appearance of an evanescent operator is at three loops which was originally observed in [14, 17]. Whilst this postdates the three loop $\overline{\text{MS}}$ β -functions of [7, 8] the latter are unaffected by the generation of \mathcal{O}_3 since it occurs with a coupling dependence of g^3 . So that coupled with $C^{(3)}(g)$ it will only affect the β -function itself at four loops. Equally the mass anomalous dimension of [11] does not feel this evanescent operator presence until four loops either. We refrain from quoting the value of the associated β -function, $\beta_3(g)$, until later. This is primarily because there are two completing values given in [17] and [18]. In the former the renormalization was deduced in a massless version of (2.1) where it was claimed that only ladder style diagrams were the origin of \mathcal{O}_3 . In that instance the nullification of two external momenta in the associated 4-point function should not have resulted in spurious infrared singularities. Whilst a $\beta_3(g)$ was determined, it involved $\zeta(3)$ which was not found in [18] which used the massive version, (2.1), where $\zeta(x)$ is the Riemann zeta function. This clearly avoided infrared singularities when all the external momenta were nullified in the 4-point function. Moreover it was claimed that the diagrams leading to \mathcal{O}_3 were akin to those analysed in [17] but with no $\zeta(3)$ appearing in the published value of $\beta_3(g)$. Though both calculations agreed on the rational part of $\beta_3(g)$. The discrepancy between both computations needs to be resolved and a four loop calculation which requires $\beta_3(g)$ explicitly to obtain the true renormalization group function will provide a non-trivial forum in which to achieve this. The correct expression for $\beta_3(g)$ will be crucial for the four loop β -function. Given this structure of the Gross-Neveu model we can now write down the renormalized form of (2.1) we will use. It is, [17, 18],

$$L = iZ_\psi \bar{\psi}^i \not{\partial} \psi^i - mZ_\psi Z_m \bar{\psi}^i \psi^i + \frac{1}{2}g\mu^\epsilon Z_g Z_\psi^2 (\bar{\psi}^i \psi^i)^2 + \frac{1}{2}g\mu^\epsilon Z_{33} Z_\psi^2 \left(\bar{\psi}^i \Gamma_{(3)} \psi^i \right)^2 \quad (2.9)$$

where the renormalized quantities are defined from their bare counterparts by

$$\psi_0 = \psi Z_\psi^{\frac{1}{2}} \quad , \quad m_0 = mZ_m \quad , \quad g_0 = gZ_g \mu^\epsilon \quad (2.10)$$

in d -dimensions and Z_{33} absorbs the infinity associated with the generation of \mathcal{O}_3 at this order. Unlike Z_ψ , Z_m and Z_g its coupling constant expansion does not commence with unity. Though we stress that (2.9) is valid only for 2-point calculations to four loops. Only by renormalizing the 4-point function at four loops would the full evanescent operator structure at that order emerge. For instance, it is not inconceivable given the γ -matrix structure of the four loop 4-point function that a \mathcal{O}_4 evanescent operator will be generated. From these renormalization constants the naive renormalization group functions are given by

$$\begin{aligned} \tilde{\gamma}(g) &= \mu \frac{\partial}{\partial \mu} \ln Z_\psi \quad , \quad \tilde{\gamma}_m(g) = -\tilde{\beta}(g) \frac{\partial}{\partial g} \ln Z_m \\ \tilde{\beta}(g) &= (d-2)g - g \tilde{\beta}(g) \frac{\partial}{\partial g} \ln Z_g \end{aligned} \quad (2.11)$$

to the order we are working to. For $\beta_3(g)$ one deduces its explicit form from the simple pole in ϵ via standard methods, [14]. Thus in the context of (2.8) and these observations, we note that for the mass anomalous dimension the result of [18] for $\rho_m^{(3)}(g)$ is

$$\rho_m^{(3)}(g) = -\frac{g}{\pi} + O(g^2) \quad . \quad (2.12)$$

The higher terms are not required since the first term of $\beta_3(g)$ is $O(g^3)$.

3 Three loop calculations.

We begin this section by discussing the computational strategy. To determine the mass anomalous dimension for (2.1) we consider the 2-point function for the massive theory. In [9] the four loop $\overline{\text{MS}}$ anomalous dimension was calculated and independently verified in [10]. Therefore, we assume that result for Z_ψ . However, this is effectively a three orders calculation since the one loop snail of Figure 1 corresponding to $\langle \psi_\alpha(p) \bar{\psi}^\beta(-p) \rangle$ has no non-zero contributions in the \not{p} channel for the massive or massless Lagrangians where p is the external momentum. Moreover, since for this case one is interested only in Z_ψ , it sufficed to consider the *massless* theory whence one only has to determine massless Feynman integrals. The component involving \not{p}_α^β can be deduced by multiplying all diagrams by \not{p} and taking the spinor trace. For the mass dimension one cannot follow this strategy. Not only because the one loop diagram contributes but also because its contribution to Z_m requires the presence of the mass itself. Therefore unlike the determination of Z_ψ one cannot neglect the snail graph of Figure 1 at one loop as well as the graphs where snails appear as subgraphs at higher order. However, given that one is only interested in the $m\delta_\alpha^\beta$ channel of $\langle \psi_\alpha(p) \bar{\psi}^\beta(-p) \rangle$ the Green's function can be analysed by nullifying the external momentum. Taking the spinor trace produces Lorentz scalar integrals but with tensor structure resulting from internal momenta contractions. The presence of the common mass m automatically protects against the appearance of spurious infrared infinities and relegates the problem of determining the ultraviolet structure to mapping the integrals with internal momenta contractions to a set of basic master vacuum bubbles at each loop order. The problem of studying massive vacuum bubbles in *four* dimensions has received much attention over the years, culminating in, for example, the MATAD package at three loops, [24], and the comprehensive study by Broadhurst of all combinations of massive and massless propagators in the Benz or tetrahedron topology, [25]. The analogous problem relative to two dimensions has not been treated as systematically. Though the main results to three loops have appeared within various articles. Additionally, at four loops we will have to handle new integrals for topologies which do not simply break into products of lower loop vacuum bubbles. The main difficulty lies in having to handle the tensor structure emanating from the fermion propagator. Throughout we have made extensive use of the symbolic manipulation language FORM, [12], in which to code our algorithm where the contributing Feynman diagrams to the 2 and 4-point functions are generated automatically with the QGRAF package, [23]. To summarize there are 1 one loop, 2 two loop, 7 three loop and 36 four loop graphs for the 2-point function. For the 4-point function there are 3 one loop, 18 two loop and 138 three loop graphs to renormalize.

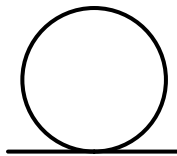


Figure 1: One loop contribution to the 2-point function.

At three loops we now summarize the few master (massive) integrals which will be of interest to us, in our notation and conventions. First, Figure 2 denotes the basic vacuum bubbles to two loops. We define the first graph of Figure 2 as

$$I = i \int_k \frac{1}{[k^2 - m^2]} . \quad (3.1)$$

We work in Minkowski space and choose to include a factor of i with each integration measure which is abbreviated by

$$\int_k = \int \frac{d^d k}{(2\pi)^d} . \quad (3.2)$$

The integral I is trivial to deduce from the Euler β -function as

$$I = \frac{\Gamma(1 - d/2)}{(4\pi)^{d/2}} (m^2)^{d/2-1} . \quad (3.3)$$

Hence the middle graph of Figure 2 is I^2 .

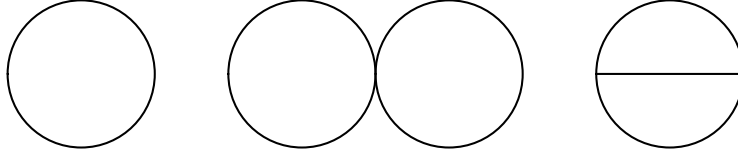


Figure 2: One and two loop vacuum bubbles.

The final graph we denote by $\Delta(0)$, [11], where

$$\Delta(0) = i \int_k \frac{J(k^2)}{[k^2 - m^2]} \quad (3.4)$$

and

$$J(p^2) = i \int_k \frac{1}{[k^2 - m^2][(k-p)^2 - m^2]} \quad (3.5)$$

is the basic one loop self-energy bubble. There is a sequence of integrals related to $J(p)$ defined by

$$J_{\alpha\beta}(p) = i \int_k \frac{1}{[k^2 - m^2]^\alpha [(k-p)^2 - m^2]^\beta} \quad (3.6)$$

where we choose $J_{21}(p) \equiv K(p^2)$. In this form a Gauss relation of the hypergeometric functions gives the relation

$$(p^2 - 4m^2)K(p^2) = J(0) - (d-3)J(p^2) \quad (3.7)$$

with

$$J(0) = - \frac{\Gamma(2 - d/2)}{(4\pi)^{d/2}} (m^2)^{d/2-2} \quad (3.8)$$

since explicit calculations produce

$$J(p^2) = - \frac{\Gamma(2 - d/2)}{(4\pi)^{d/2}} \left(\frac{4m^2 - p^2}{4} \right)^{d/2-2} {}_2F_1 \left(2 - \frac{d}{2}, \frac{1}{2}; \frac{3}{2}; \frac{p^2}{p^2 - 4m^2} \right) \quad (3.9)$$

and

$$K(p^2) = \frac{\Gamma(3 - d/2)}{2(4\pi)^{d/2}} \left(\frac{4m^2 - p^2}{4} \right)^{d/2-3} {}_2F_1 \left(3 - \frac{d}{2}, \frac{1}{2}; \frac{3}{2}; \frac{p^2}{p^2 - 4m^2} \right) . \quad (3.10)$$

Likewise, at the subsequent level

$$(p^2 - 4m^2) (J_{22}(p^2) + 2J_{31}(p^2)) = 2K(0) - 2(d-5)K(p^2) \quad (3.11)$$

whence

$$\begin{aligned} J_{31}(p^2) &= \frac{(d-6)}{2p^2} K(p^2) + \frac{(p^2 - 2m^2)}{p^2(p^2 - 4m^2)} \left(K(0) - (d-5)K(p^2) \right) \\ J_{22}(p^2) &= -\frac{(d-6)}{p^2} K(p^2) + \frac{4m^2}{p^2(p^2 - 4m^2)} \left(K(0) - (d-5)K(p^2) \right) . \end{aligned} \quad (3.12)$$

These rules are used extensively for the two and higher loop Feynman integrals. The integral $\Delta(0)$ is finite in two dimensions and can be evaluated in an expansion in powers of ϵ as

$$\Delta(0) = -\frac{9s_2}{16\pi^2 m^2} + O(\epsilon) \quad (3.13)$$

where $s_2 = (2\sqrt{3}/9)\text{Cl}_2(2\pi/3)$ with $\text{Cl}_2(x)$ the Clausen function. The analogous four dimensional vacuum bubble also contains s_2 in its finite part but is divergent. In principle the $O(\epsilon)$ term of (3.13) can be deduced. However, throughout our computations we left $\Delta(0)$ itself unevaluated since on renormalizability grounds it must be absent from the final renormalization constants at higher loops. This is because if the 2-point function did not have its external momenta nullified then the integral $\Delta(p)$ would emerge, where

$$\Delta(p) = i \int_k \frac{J(k^2)}{[(k-p)^2 - m^2]} . \quad (3.14)$$

Clearly such a non-local function of the external momenta could not be retained when all the counterterms are included.

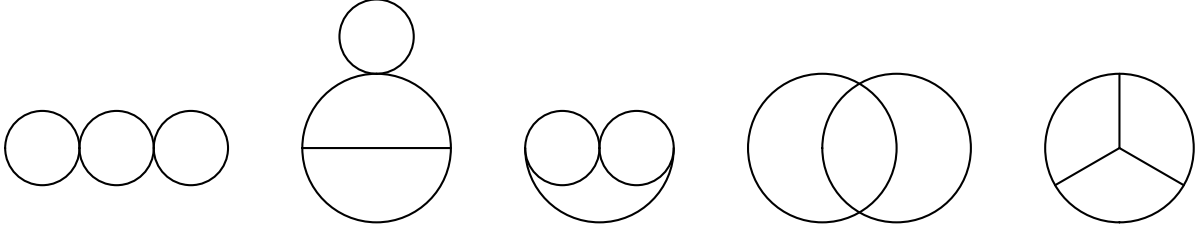


Figure 3: Three loop vacuum bubbles.

At three loops there are several more basic topologies. If one ignores for the moment the complication due to the presence of internal momenta contractions in integral numerators, then the basic graphs are given in Figure 3. The first involves I and its derivatives with respect to m^2 . Also the second is a variation on $\Delta(0)$ and we note that the two loop subgraph is

$$i \int_k \frac{J(k^2)}{[k^2 - m^2]^2} = \frac{(d-3)}{3m^2} \Delta(0) \quad (3.15)$$

which is established by differentiating $\Delta(0)$ with respect to m^2 . Aside from the Benz topology the remaining vacuum bubbles of Figure 3 are related to the integrals $i \int_k J^2(k^2)/[k^2 - m^2]$, $i \int_k J^2(k^2)$ and $i \int_k J(k^2)K(k^2)$. Similar to $\Delta(0)$ these are finite in two dimensions but their values are required at four loops when multiplied by counterterms. As only the leading term in ϵ is required in each case it transpires that we can set $d = 2$ and use the fact that in Euclidean space, denoted by the subscript E ,

$$J_E(-k^2) \Big|_{d=2} = \frac{\theta}{\sinh \theta} J(0) \Big|_{d=2} \quad (3.16)$$

upon the change of variables $k^2 = 4m^2 \sinh^2(\theta/2)$ where $J(0)|_{d=2} = -1/(4\pi m^2)$. Then, for instance,

$$i \int_k J^2(k^2) = - \frac{m^2}{2\pi} J^2(0)|_{d=2} \int_0^\infty d\theta \frac{\theta^2}{\sinh \theta} + O(\epsilon) . \quad (3.17)$$

This can be evaluated from standard integrals to give

$$i \int_k J^2(k^2) = - \frac{7\zeta(3)}{64\pi^3 m^2} + O(\epsilon) . \quad (3.18)$$

Equally we find

$$i \int_k \frac{J^2(k^2)}{[k^2 - m^2]} = \frac{11\zeta(3)}{576\pi^3 m^4} + O(\epsilon) . \quad (3.19)$$

Though in d -dimensions one can derive the relation

$$i \int_k J(k^2) K(k^2) = \frac{(3d-8)}{8m^2} i \int_k J^2(k^2) . \quad (3.20)$$

The presence of $K(k^2)$ in several of the master integrals with topology similar to those of Figure 3 produces similar finite integrals whose finite part is required and which is determined in an analogous way. We note that

$$\begin{aligned} i \int_k \frac{J(k^2)}{[k^2 - 4m^2]} &= \frac{\ln(2)}{2\pi} J(0)|_{d=2} + O(\epsilon) \\ i \int_k \frac{J^2(k^2)}{[k^2 - 4m^2]} &= \left[\frac{7}{8} \zeta(3) - \ln(2) \right] \frac{J^2(0)}{2\pi} \Big|_{d=2} + O(\epsilon) . \end{aligned} \quad (3.21)$$

For the mass anomalous dimension these basic vacuum bubbles suffice to determine the renormalization constants to three loops. Given the nature of the 4-point interaction in (2.1) the Benz topology does not occur in the 2-point function at this loop order.

Having discussed the basic scalar master integrals which result we briefly note the algorithm dealing with the numerator structure of the integrals. This has been systematically quantified in [11]. However, we note that repeated use of

$$kl = \frac{1}{2} \left[k^2 + l^2 - [(k-l)^2 - m^2] - m^2 \right] \quad (3.22)$$

and then

$$k^2 = [k^2 - m^2] + m^2 , \quad l^2 = [l^2 - m^2] + m^2 \quad (3.23)$$

in each contributing topology where there are $[k^2 - m^2]$, $[l^2 - m^2]$ and $[(k-l)^2 - m^2]$ propagators already. This is done in such a way that powers of kl can remain when all mixed $[(k-l)^2 - m^2]$ propagators are absent and one does not then continue substituting for kl . In such integrals one can use Lorentz symmetry in the k and l subgraph integrals to redefine even powers of kl as proportional to $k^2 l^2$ or zero if there are an odd number of factors of kl . Then (3.23) is repeated. Consequently several variations in the basic bubble graphs of Figure 3 emerge and we note that

$$\begin{aligned} i \int_k k^2 J^2(k^2) &= \frac{4}{3} I^3 + \frac{4}{3} m^2 i \int_k J^2(k^2) \\ i \int_k (k^2)^2 J^2(k^2) &= \frac{8m^2}{3(3d-4)} \left[(5d-6) I^3 + 2dm^2 i \int_k J^2(k^2) \right] \end{aligned} \quad (3.24)$$

where these are exact and no finite parts have been omitted since these are crucial for the next loop order. In essence this summarizes the key ingredients in the algorithm for evaluating the three loop mass anomalous dimension which has been coded in FORM and reproduces the previous three loop $\overline{\text{MS}}$ Gross-Neveu mass anomalous dimension.

4 Three loop 4-point function renormalization.

At this point we turn to our secondary aim which is to resolve the discrepancy in the renormalization associated with the generation of \mathcal{O}_3 . This requires the complete determination of the 4-point function divergence structure at three loops. Whilst the algorithm to do this is very similar to that of the 2-point function there are several key differences. First, the 4-point function divergences will be independent of the external momenta which means that they can be immediately nullified. The mass again protects against spurious infrared divergences. However, we cannot now take the Lorentz traces since that would prevent one from seeing the emergence of any $\Gamma_{(3)}^{\mu\nu\sigma} \otimes \Gamma_{(3)\mu\nu\sigma}$ γ -matrix structure. Instead we have to retain γ -strings and also unentangle the internal momenta within them. Hence one decouples the Feynman diagrams into γ -strings and Lorentz tensor vacuum bubbles. At one and two loops the resulting tensor integrals for the whole integral can be straightforwardly reduced by noting that at one loop

$$\int_k k^\mu k^\nu f_1(k^2) = \frac{\eta^{\mu\nu}}{d} \int_k k^2 f_1(k^2) \quad (4.1)$$

where k is the sole loop momentum and at two loops

$$\begin{aligned} \int_{kl} k_1^{\mu_1} k_2^{\mu_2} k_3^{\mu_3} k_4^{\mu_4} f_2(k, l) &= \frac{1}{d(d-1)(d+2)} \\ &\int_{kl} f_2(k, l) [(d+1)k_1.k_2k_3.k_4 - k_1.k_3k_2.k_4 - k_1.k_4k_2.k_3] \eta^{\mu_1\mu_2} \eta^{\mu_3\mu_4} \\ &+ [(d+1)k_1.k_3k_2.k_4 - k_1.k_2k_3.k_4 - k_1.k_4k_2.k_3] \eta^{\mu_1\mu_3} \eta^{\mu_2\mu_4} \\ &+ [(d+1)k_1.k_4k_2.k_3 - k_1.k_2k_3.k_4 - k_1.k_3k_2.k_4] \eta^{\mu_1\mu_4} \eta^{\mu_2\mu_3} \end{aligned} \quad (4.2)$$

where $k_i \in \{k, l\}$ and in the Lorentz tensor of the integrand all possible combinations of the two internal momenta are covered. The functions $f_i(\{k_i\})$ represent the various possible propagator combinations. For clarity we have included the dot of the scalar products explicitly. At three loops the situation is complicated by the observation that the extension of both these formula gives

$$\begin{aligned} \int_{klq} k_1^{\mu_1} k_2^{\mu_2} k_3^{\mu_3} k_4^{\mu_4} k_5^{\mu_5} k_6^{\mu_6} f_3(k, l, q) &= \frac{\eta^{\mu_1\mu_2} \eta^{\mu_3\mu_4} \eta^{\mu_5\mu_6}}{d(d-1)(d-2)(d+2)(d+4)} \\ &\int_{klq} f_3(k, l, q) [(d^2 + 3d - 2)k_1.k_2k_3.k_4k_5.k_6 \\ &- (d+2)k_1.k_2k_3.k_5k_6.k_4 - (d+2)k_1.k_2k_3.k_6k_4.k_5 \\ &- (d+2)k_1.k_3k_2.k_4k_5.k_6 + 2k_1.k_3k_2.k_5k_6.k_4 \\ &+ 2k_1.k_3k_2.k_6k_4.k_5 - (d+2)k_1.k_4k_2.k_3k_5.k_6 \\ &+ 2k_1.k_4k_2.k_5k_6.k_3 + 2k_1.k_4k_2.k_6k_3.k_5 \\ &+ 2k_1.k_5k_2.k_3k_4.k_6 + 2k_1.k_5k_2.k_4k_6.k_3 \\ &- (d+2)k_1.k_5k_2.k_6k_3.k_4 + 2k_1.k_6k_2.k_3k_4.k_5 \\ &+ 2k_1.k_6k_2.k_4k_5.k_3 - (d+2)k_1.k_6k_2.k_5k_3.k_4] \\ &+ 14 \text{ similar terms} \end{aligned} \quad (4.3)$$

where $k_i \in \{k, l, q\}$. The full decomposition is clearly quite large. However, it is the appearance of the $1/(d-2)$ factor which is novel. In [17, 18] the full set of three loop graphs in both massless and massive cases where a divergent $\Gamma_{(3)}^{\mu\nu\sigma} \otimes \Gamma_{(3)\mu\nu\sigma}$ structure emerged, was noted. The sets of graphs appear to be the same. Though in [17] it is not fully clear which the actual ladder graphs

referred to are. However, the seemingly *finite* graph of Figure 4 was regarded as fully finite in *all* γ -string channels, [18]. In our present reconsideration it transpires that within the integral of the graph of Figure 4 there is a divergent contribution to the $\Gamma_{(3)}^{\mu\nu\sigma} \otimes \Gamma_{(3)}{}_{\mu\nu\sigma}$ channel but *not* for the $\Gamma_{(0)} \otimes \Gamma_{(0)}$ one. This derives from the pole $1/(d-2)$ in (4.3) producing the massive Benz integral corresponding to the final graph of Figure 3. The key part is then

$$\frac{1}{(d-2)} \int_{klq} \frac{1}{[k^2 - m^2][l^2 - m^2][q^2 - m^2][(k-l)^2 - m^2][(k-q)^2 - m^2][(l-q)^2 - m^2]} \quad (4.4)$$

where the actual integral itself is finite in two dimensions. It remains after repeated application of (3.22) and (3.23) in the scalar integrals of (4.3). However, to have the complete divergence structure the integral needs to be evaluated since it will contribute to Z_{33} . The remaining integrals with this $1/(d-2)$ pole in the $\Gamma_{(3)}^{\mu\nu\sigma} \otimes \Gamma_{(3)}{}_{\mu\nu\sigma}$ channel correspond to (4.4) but with one or more propagators removed after application of (3.22) and (3.23). These can be evaluated from the three loop techniques discussed earlier. In [18] this contribution, (4.4), was overlooked since it was assumed that the parent integral with the internal momenta contracted was finite without noting the possibility of the $1/(d-2)$ factor deriving from the tensor decomposition. In relation to [17] we can only comment that in the massless version of (4.4) the integral will be zero. However, given the totally different method of calculating the 4-point function of [18] in the massless case, a contribution analogous to (4.4) could possibly arise elsewhere.

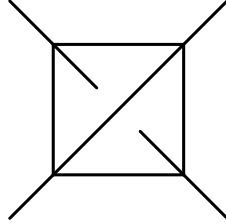


Figure 4: Three loop contribution to 4-point function.

There remains the task now of evaluating the *integral* of (4.4). Although finite it clearly cannot be reduced to any of the three loop master vacuum bubbles already discussed even using, say, integration by parts. Instead we have had to resort to the more extensive experience of four dimensional vacuum bubble diagrams and specifically the Benz graphs discussed in [25]. To promote (4.4) to four dimensions we exploit Tarasov's observation of relating d -dimensional integrals to $(d+2)$ -dimensional ones, [26, 27]. Moreover, this is straightforward to do via the TARCER package, [28], written in MATHEMATICA for the basic two loop self energy topology given in Figure 5. Specifically one feature of TARCER is that one can relate this two loop self energy graph in d -dimensions to that in $(d+2)$ -dimensions. This is a subgraph of Figure 4 with nullified external momenta and given that this is a three loop vacuum bubble, the final three loop integration measure can be rewritten as

$$\int \frac{d^d k}{(2\pi)^d} = 2\pi d \int \frac{d^{d+2} k}{(2\pi)^{d+2}} \frac{1}{k^2} \quad (4.5)$$

in our conventions since the two loop subgraph will clearly be a function of k^2 only. From (4.5) a massless propagator will appear in the higher dimensional integral. Since all the lines of Figures 4 and 5 are massive and both final integrations involve functions of the square of the momentum, then we find the relation between the d -dimensional massive Benz graph and similar topologies

in two dimensions higher is

$$\begin{aligned}
& \text{Be}(1, 1, 1, 1, 1, 1, m^2, m^2, m^2, m^2, m^2, d) \\
&= -\frac{1}{12m^4} i \int_k J^2(k^2) - \frac{3}{4m^2} i \int_k \frac{J^2(k^2)}{[k^2 - m^2]} \\
&\quad + \frac{\pi d(d-1)(d-2)}{m^6} \left[\text{Be}(1, 1, 1, 1, 1, 1, m^2, m^2, m^2, m^2, m^2, d+2) \right. \\
&\quad \left. - \text{Be}(1, 1, 1, 1, 1, 1, 0, m^2, m^2, m^2, m^2, d+2) \right] \quad (4.6)
\end{aligned}$$

where we define

$$\begin{aligned}
& \text{Be}(\alpha, \beta, \gamma, \rho, \lambda, \theta, m_1^2, m_2^2, m_3^2, m_4^2, m_5^2, m_6^2, d) \\
&= i^3 \int_{klq} \frac{1}{[k^2 - m_1^2]^\alpha [l^2 - m_2^2]^\beta [q^2 - m_3^2]^\gamma [(k-l)^2 - m_4^2]^\rho [(k-q)^2 - m_5^2]^\lambda [(l-q)^2 - m_6^2]^\theta} \quad (4.7)
\end{aligned}$$

and emphasise that \int_k indicates a d -dimensional integration. The key part is the piece which represents the difference in two Benz topologies in $(d+2)$ -dimensions where one is completely massive and the other has one massless line. However, since these are multiplied by $(d-2)$ then in our ϵ expansion relative to two dimensions we note that the leading term of each is $O(\epsilon)$ meaning that

$$\begin{aligned}
& i^3 \int_{klq} \frac{1}{[k^2 - m^2][l^2 - m^2][q^2 - m^2][(k-l)^2 - m^2][(k-q)^2 - m^2][(l-q)^2 - m^2]} \\
&= -\frac{\zeta(3)}{192\pi^3 m^6} + O(\epsilon) \quad (4.8)
\end{aligned}$$

from (3.18) and (3.19). This is because whilst each of the two $(d+2)$ -dimensional integrals are divergent in four dimensions due to the presence of a simple pole in the regularizing parameter, the difference in (4.6) is finite and the residue is independent of the masses in either Benz topology, [25].

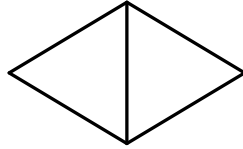


Figure 5: Two loop self-energy topology central to TARCER.

With this observation all the ingredients are assembled to repeat the full three loop renormalization of the 4-point function of (2.1). In [7] only the $\Gamma_{(0)} \otimes \Gamma_{(0)}$ part was isolated but this was sufficient to deduce the β -function at three loops. It is satisfying to record that we have verified the previous three loop $\overline{\text{MS}}$ result of [7, 8]. However, by contrast we find that a different renormalization constant from [17] and [18] emerges for Z_{33} . We find

$$Z_{33} = \left[\frac{\zeta(3)}{64} - \frac{1}{48} \right] \frac{g^3}{\pi^3 \epsilon} + O(g^4) \quad (4.9)$$

whence

$$\beta_3(g) = \left[\frac{3\zeta(3)}{64} - \frac{1}{16} \right] \frac{g^3}{\pi^3} + O(g^4). \quad (4.10)$$

Though there is universal agreement on the rational part of (4.10), [17, 18], only the contribution from the diagram of Figure 5 to the $\Gamma_{(3)}^{\mu\nu\sigma} \otimes \Gamma_{(3)}{}_{\mu\nu\sigma}$ channel produces the irrational piece thereby confirming the overall structure observed in [17]. However, rather than finding that we produce one of the previous values for Z_{33} we are in the seemingly unfortunate position of finding a new alternative. To determine which is correct and consistent it will transpire that the four loop mass anomalous dimension is the correct testing ground for this in the context of (2.8).

5 Four loop vacuum bubbles.

In this section we return to our initial aim and summarize the evaluation of the underlying four loop vacuum bubbles required for the mass anomalous dimension. For the 2-point function there are 18 distinct topologies and 36 Feynman diagrams to be considered. Of these topologies 14 involve snail insertions in one way or another and hence their determination is in effect relegated to the straightforward extension of the three loop topology discussion. One effect of a snail is to produce two propagators on a line of a three loop graph but this can be reproduced by differentiating that line with respect to m^2 . This is also a reason why the three loop vacuum bubbles were required to be evaluated to the finite part exactly or left in terms of $\Delta(0)$ and other known integrals whose ϵ expansion could be substituted when required, if at all. Several topologies contributing to the 2-point function, however, have a more demanding evaluation. These are illustrated in Figure 6 and we concentrate on these for the main part. Essentially the main complication now derives from rewriting the scalar products of internal momenta in terms of the propagator structure. For all the integrals which result we used several interconnected techniques.

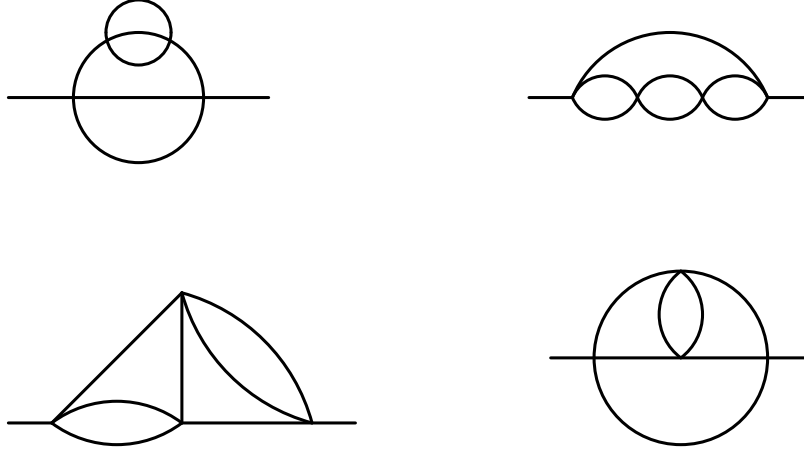


Figure 6: Several four loop diagrams contributing to the 2-point function.

First was the use of the TARCER package, [28], again, particularly for the third and fourth graphs of Figure 6. Clearly the last graph contains the two loop self-energy topology of Figure 5 as a subgraph and the third has a similar two loop subgraph but with one line removed. Unlike the properties of TARCER we described previously, the feature exploited in this instance is the ability to relate diagrams with different powers of the propagators in Figure 5 to that with unit power. Further, TARCER reduces integrals involving powers of the scalar products kl , kp and lp where k and l are internal and p is the external momentum in Figure 5. The point is that the Lorentz tensor reduction for these situations can only be performed by this route. Any one

loop subgraph of Figure 5 will involve three external legs and the invariant decomposition in this case is too intricate. By contrast where possible we did exploit the Lorentz structure of subgraphs with *one* internal momentum flowing through it which can be regarded as a 2-point function external momentum for that subgraph. Then integrals can be rewritten using results such as

$$i \int_l \frac{l^\mu l^\nu}{[l^2 - m^2][(k-l)^2 - m^2]} = \frac{1}{(d-1)} i \int_l \frac{1}{[l^2 - m^2][(k-l)^2 - m^2]} \times \left[\eta^{\mu\nu} \left(l^2 - \frac{k l^2}{k^2} \right) - \frac{k^\mu k^\nu}{k^2} \left(l^2 - d \frac{k l^2}{k^2} \right) \right]. \quad (5.1)$$

The outcome of the TARCER implementation is to reduce these more complicated tensor integrals to a set of master scalar four loop vacuum bubbles since the resulting combination of internal momenta allows for the repeated application of (3.22) and (3.23).

The use of (5.1) and TARCER though may appear to introduce potential infrared difficulties. However, it transpires that in the full sum of all contributing pieces to a Feynman graph it can be checked that no integral retains an unprotected factor of $1/k^2$ which would give an infrared divergence upon integrating over the internal momentum k . For one instance checking this proved to be a tedious non-trivial exercise which we document for completeness. In all bar the second graph of Figure 6 the following combination of integrals emerge

$$V_\Delta = i \int_k \left[J(k^2) - J(0) \right] \frac{\Delta(k)}{k^2}. \quad (5.2)$$

Clearly each could be infrared divergent but the above combination always appears. Defining

$$K_\mu(p) = i \int_k \frac{k_\mu}{[k^2 - m^2]^2 [(k-p)^2 - m^2]} \quad (5.3)$$

then one can show

$$p^\mu K_\mu(p) = 2m^2 K(p^2) - \frac{1}{2}(d-4)J(p^2) = \frac{1}{2} \left[p^2 K(p^2) + J(p^2) - J(0) \right]. \quad (5.4)$$

Using this and integration parts in (5.3) one finds

$$V_\Delta = (d-3)i \int_k \frac{1}{k^2} J(k^2) \Delta(k^2) - 2i \int_k \Delta(k) K(k^2) + i^2 \int_{kl} \frac{(k^2 - m^2) J(k^2) J(l^2)}{l^2 [(k-l)^2 - m^2]^2}. \quad (5.5)$$

The final integral can be reduced using TARCER if one regards the k momentum as external to the self-energy graph of Figure 5 and $J(l^2)$ is replaced by the Feynman integral of (3.5). Consequently, TARCER produces

$$\begin{aligned} i \int_l \frac{J(l^2)}{l^2 [(k-l)^2 - m^2]^2} &= \frac{(d-2)^2 (d-4) I^2}{2(d-3)m^2 [k^2 - m^2]^2} - \frac{(d-2)(d-3)}{2m^2 [k^2 - m^2]} i \int_l \frac{1}{l^2 [(k-l)^2 - m^2]} \\ &+ \frac{(d-4)(3d-8)}{[k^2 - m^2]^2} i^2 \int_{lq} \frac{1}{[l^2 - m^2][(k-q)^2 - m^2][(l-q)^2 - m^2]} \\ &+ \frac{[(d-2)[k^2 - m^2] - 8(d-4)m^2}{[k^2 - m^2]^2} \\ &\times i^2 \int_{lq} \frac{1}{[l^2 - m^2]^2 [(k-q)^2 - m^2][(l-q)^2 - m^2]}. \end{aligned} \quad (5.6)$$

The benefit of rearranging the two loop integral of the left hand side is to isolate the potential infrared singularity into a simple term on the right hand side. Moreover, the appearance of

powers of $1/[k^2 - m^2]$ will lead to simplifications when substituted back into the expression for V_Δ and the term with the singularity will actually combine with the first term of (5.5) to produce V_Δ but with a factor of $(d - 3)$. Hence, evaluating the remaining integrals of (5.6) in the context of (5.5) one arrives at the expression

$$\begin{aligned} V_\Delta = & -i \int_k \Delta(k) K(k^2) - \frac{(d-2)^2 I^2 \Delta(0)}{2(d-3)m^2} \\ & - (3d-8)i \int_k \frac{J(k^2) \Delta(k)}{[k^2 - m^2]} + 8m^2 i^2 \int_{kl} \frac{J(k) K(l)}{[k^2 - m^2][(k-l)^2 - m^2]} \end{aligned} \quad (5.7)$$

which has no potential infrared singular term. Moreover, each term of the right side of this is ultraviolet finite in two dimensions. So, in fact, when the combination V_Δ appears in our computation, it can actually be dropped as there is no contribution to the renormalization of the mass at four loops.

Having completed the tensor reduction of the scalar propagators, all that remains is the evaluation of a set of divergent four loop master integrals akin to those discussed earlier. Most of these are elementary given the results of (3.7), (3.11) and (3.12) and the observation that as all integrals are infrared finite then one can ignore those four loop ones which are clearly ultraviolet finite by the usual counting rules. Though one integral is worth recording and that is

$$i \int_k (k^2)^2 J^3(k^2) = 2I^4 + \frac{(7d-13)m^2 I}{(2d-5)} i \int_k J^2(k^2) + \frac{2(d-1)(d-3)}{(2d-5)(d-2)} m^4 i \int_k J^3(k^2) \quad (5.8)$$

because in the determination of this relation a pole in $(d-2)$ emerges in the standard d -dimensional manipulations such as differentiating the original integral with respect to m^2 and using (3.7). This pole gives rise to a problem similar to that discussed for (4.4) but with a simpler resolution since we merely apply the technique used to deduce (3.18) and (3.19), to find

$$i \int_k J^3(k^2) = \frac{3\zeta(3)}{256\pi^4 m^4} + O(\epsilon). \quad (5.9)$$

The need to evaluate $i \int_k J^2(k^2)$ to the finite part as well is also illustrated by this equation.

This completes the discussion of the construction of the relevant basic Feynman integrals. For each of the eighteen topologies a FORM module was created within which the algorithm to break the original Feynman graphs up into its basic components was encoded. The tedious identification with the above results together with the remaining more elementary ones were also contained in each module. Finally, prior to summing all the results from the 36 four loop diagrams, the ϵ expansion of I and other integrals were evaluated to the appropriate order in ϵ . The resulting sum produced the divergent part of the mass component of the 2-point function to the simple pole in ϵ as a function of the bare parameters.

6 Four loop renormalization.

The final piece of the calculation rests in determining the overall renormalization constant Z_m at four loops in $\overline{\text{MS}}$. However, prior to this we must consider the full theory. To this point we have tacitly assumed that only the basic 4-point vertex of (2.1) is responsible for all the Feynman diagrams we have discussed. The presence of the generated evanescent operator in (2.9) needs to be included. As noted earlier since the operator appears with a coupling g^4 the effect of this operator cannot arise before four loops. Therefore, we now have to include the additional graph

of Figure 7 where the circle with a cross in it denotes the insertion of the operator \mathcal{O}_3 with its associated renormalization constant Z_{33} . The integration routine to determine its contribution is the same as that for the original vertex except that one has to first replace the $\Gamma_{(3)}^{\mu\nu\sigma}$ matrices by the corresponding string of ordinary γ -matrices.

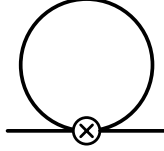


Figure 7: Contribution from evanescent operator to the four loop mass renormalization.

With this additional graph included the overall renormalization constant is extracted using the standard method for automatic Feynman diagram computations developed in [29]. Briefly one computes the Green's function of interest as a function of all the bare parameters such as the coupling constant and the mass. Then the renormalized parameters are introduced by the rescaling defined by the renormalization constants. In the present context these are the renormalization constants leading to the *naive* anomalous dimensions as defined in (2.9) and (2.10). This rescaling in effect reproduces the counterterms to remove subgraph divergences. Moreover the Green's function is multiplied by the associated renormalization constant which in our case and conventions is $Z_\psi Z_m$. As the former is already known, [9], then the divergences which remain in the 2-point function are absorbed by the unknown pieces of Z_m . We recall that at four loops the anomalous dimension of [9] corresponds to the naive anomalous dimension $\tilde{\gamma}(g)$ since there is no contribution from the graph of Figure 7 in the wave function channel. Therefore, having followed this procedure we find the naive mass anomalous dimension in $\overline{\text{MS}}$ is

$$\begin{aligned} \tilde{\gamma}_m(g) = & - (2N - 1) \frac{g}{2\pi} + (2N - 1) \frac{g^2}{8\pi^2} + (4N - 3)(2N - 1) \frac{g^3}{32\pi^3} \\ & + \left[(48N^3 - 384N^2 + 492N - 138)\zeta(3) - 40N^3 - 72N^2 + 160N - 81 \right] \frac{g^4}{384\pi^4} \\ & + O(g^5) . \end{aligned} \tag{6.1}$$

At this stage several comments are necessary. First, there are several checks on the underlying renormalization constant itself. Whilst the evanescent operator issue arises at four loops, it will manifest itself in the simple pole in ϵ of Z_m . Therefore, the quartic, triple and double poles in ϵ are in fact already predetermined by the structure of previous loop order poles from the renormalization group equation. For (6.1) we have verified that this is in fact correct. One other useful check was the explicit cancellation of divergences of the form $\Delta(0)/\epsilon^n$ for $n = 1$ and 2 at four loops. This is non-trivial since, for instance, $\Delta(0)$ arises at three loops both associated with a simple pole in ϵ and in the finite part. Therefore, one needs to write $\Delta(0)$ as a formal expansion in powers of ϵ prior to the rescaling of the bare quantities. This is because the $O(1)$ piece at three loops will be multiplied by $1/\epsilon$ poles. Moreover, since $\Delta(0)$ has dependence $(m^2)^{d-3}$, then this has to be explicitly factored off since this mass is bare and needs to be renormalized too. Once written in this way we have checked that the poles in ϵ involving the $O(1)$ and $O(\epsilon)$ residues stemming from the ϵ expansion of $\Delta(0)$ do indeed cancel completely.

Again one can partially check part of (6.1) from another point of view. In [9] the structure of the mass anomalous dimension has been given in the large N expansion to $O(1/N^2)$ based on the results from a series of articles [30, 31, 32, 33, 34, 35, 36]. Again at this level of expansion the

evanescent operator is not manifested and so the $O(1/N^2)$ coefficients of the mass anomalous dimension which are given there at four and higher loops in fact equate to those of the naive mass anomalous dimension $\tilde{\gamma}_m(g)$. In other words if it were possible to compute the critical exponent corresponding to the mass anomalous dimension at the d -dimensional fixed point of the theory at the next order in large N , $O(1/N^3)$, then unless the effect of the evanescent operator could be included, it would not correspond to the true mass anomalous dimension, [9]. From the expression given in [9] we note that when the same convention is used, that part of (6.1) at four loops which corresponds to the $O(1/N^2)$ piece agrees precisely with [9]. This is a reassuring cross-check on a significant part of our four loop computation since, within the computer setup, one can examine the N -dependence multiplying all the basic integrals which we have had to compute for all topologies. The vast majority are at least touched by a quadratic or cubic in N which are related respectively to the $O(1/N^2)$ or $O(1/N)$ large N piece already determined in [9]. For the small number of remaining pieces which have linear factors in N we have been careful in evaluating the corresponding, though invariably simple, vacuum bubbles. Therefore, we are confident that (6.1) is correct.

One clear problem remains which is related to the structure of the expression (6.1). Unlike the previous orders the four loop part does not vanish when $N = \frac{1}{2}$ which corresponds to the free field theory. Moreover, it transpires that of the eighteen underlying topologies only the graphs for one do not vanish for this value for N . (Though actually the parts from the second and third graphs of Figure 6 cancel between each other which is similar to what occurs at three loops for analogous graphs.) The topology which gives a contribution for $N = \frac{1}{2}$ is the final graph of Figure 6. However, given our discussion in several places concerning the evanescent operator, the resolution is clearly straightforward. More concretely one can see the evidence for this if one evaluates (6.1) at $N = \frac{1}{2}$ to find

$$\tilde{\gamma}_m(g) \Big|_{N=\frac{1}{2}} = [3\zeta(3) - 4] \frac{g^4}{64\pi^4} + O(g^5) . \quad (6.2)$$

This is the piece which needs to be cancelled in order to have a mass dimension consistent with a free field theory. Indeed this is the relative combination of rationals and $\zeta(3)$ which our three loop 4-point function renormalization reevaluation produced. Therefore, using (2.8) and (4.10) we can derive the true mass anomalous dimension as

$$\begin{aligned} \gamma_m(g) = & - (2N - 1) \frac{g}{2\pi} + (2N - 1) \frac{g^2}{8\pi^2} + (4N - 3)(2N - 1) \frac{g^3}{32\pi^3} \\ & + \left[12(2N - 13)(N - 1)\zeta(3) - 20N^2 - 46N + 57 \right] (2N - 1) \frac{g^4}{384\pi^4} \\ & + O(g^5) . \end{aligned} \quad (6.3)$$

Clearly this has the correct expected $N = \frac{1}{2}$ property and given our earlier checks on (6.1) we will regard (6.3) as the completion of our original aim. Also, it is worth stressing that the discrepancy in the 4-point function renormalization has now been crucially resolved simultaneously. It turns out that neither of the previous expressions for $\beta_3(g)$, [17, 18], could be correct to preserve the vanishing of $\gamma_m(g)$ in the free field case. So we can regard this mass anomalous dimension calculation as also a non-trivial check on the full *three* loop $\overline{\text{MS}}$ renormalization.

7 Discussion.

We have completed the four loop renormalization of the mass anomalous dimension of the Gross-Neveu model in the $\overline{\text{MS}}$ scheme. Despite the lack of multiplicative renormalizability when the

Lagrangian is regularized dimensionally, it has been possible to compute an expression which passes all possible internal checks. Not least of these is the correct implementation of the projection formula formalism of [13, 14] which has been justified by the consistency with the free field case. Concerning this the previous attempts to deduce $\beta_3(g)$ appear to indicate that the only approach which is truly reliable for renormalizing the model is the one where there is a non-zero mass. This seems to be the conclusion one must draw from the origin of the necessary $\zeta(3)$ part missing from [17] required to balance the discrepancy of (6.2). Given these remarks one possible extension would now be to repeat the derivation of the mass anomalous dimension at four loops in other 4-fermi models in two dimensions. Whilst considering the most general possible interactions involving \mathcal{O}_0 , \mathcal{O}_1 and \mathcal{O}_2 of [13, 14] would perhaps be too ambitious, there is the interesting case of the non-abelian Thirring model, [37, 38]. The seed interaction involves \mathcal{O}_1 but includes colour group generators too. It has been renormalized at three loops in $\overline{\text{MS}}$ in [18] and the four loop wave function is also known, [10]. Though in light of our comments on the 4-point function in the Gross-Neveu model, the corresponding 4-point function renormalization would clearly need to be reconsidered to deduce the correct evanescent operator β -functions. One motivation for determining the mass anomalous dimension in the non-abelian Thirring model would be to examine the colour group Casimir structure of the final expression since, given the similarity with QCD, it is thought that it should involve the same structures as the corresponding expression for the quark mass anomalous dimension, [39, 40]. This was the case for the wave function, [10].

Acknowledgements. The author thanks the Max Planck Institute for the Physics of Complex Systems, Dresden, Germany where part of this work was carried out. Also the author is grateful to Dr R. Mertig for assistance with setting up TARCER.

References.

- [1] D. Gross & A. Neveu, Phys. Rev. **D10** (1974), 3235.
- [2] A.B. Zamolodchikov & A.B. Zamolodchikov, Ann. Phys. **120** (1979), 253.
- [3] A.B. Zamolodchikov & A.B. Zamolodchikov, Nucl. Phys. **B133** (1978), 525.
- [4] P. Forgacs, F. Niedermayer & P. Weisz, Nucl. Phys. **B367** (1991), 123.
- [5] B.N. Shalaev, Phys. Rept. **237** (1994), 129.
- [6] W. Wetzel, Phys. Lett. **B153** (1985), 297.
- [7] J.A. Gracey, Nucl. Phys. **B367** (1991), 657.
- [8] C. Luperini & P. Rossi, Ann. Phys. **212** (1991), 371.
- [9] N.A. Kivel, A.S. Stepanenko & A.N. Vasil’ev, Nucl. Phys. **B424** (1994), 619.
- [10] D.B. Ali & J.A. Gracey, Nucl. Phys. **B605** (2001), 337.
- [11] J.A. Gracey, Nucl. Phys. **B341** (1990), 403.
- [12] J.A.M. Vermaseren, math-ph/0010025.
- [13] A. Bondi, G. Curci, G. Paffuti & P. Rossi, Ann. Phys. **199** (1990), 268.

- [14] A. Bondi, G. Curci, G. Paffuti & P. Rossi, Phys. Lett. **B216** (1989), 349.
- [15] A.N. Vasil'ev, M.I. Vyazovskii, S.É. Derkachov & N.A. Kivel, Theor. Math. Phys. **107** (1996), 441.
- [16] A.N. Vasil'ev, M.I. Vyazovskii, S.É. Derkachov & N.A. Kivel, Theor. Math. Phys. **107** (1996), 359.
- [17] A.N. Vasil'ev & M.I. Vyazovskii, Theor. Math. Phys. **113** (1997), 1277.
- [18] J.F. Bennett & J.A. Gracey, Nucl. Phys. **B563** (1999), 390.
- [19] M.J. Dugan & B. Grinstein, Phys. Lett. **B256** (1991), 239.
- [20] S. Herrlich & U. Nierste, Nucl. Phys. **B455** (1995), 39.
- [21] W. Zimmermann, Ann. Phys. **77** (1973), 536.
- [22] W. Zimmermann, Ann. Phys. **77** (1973), 570.
- [23] P. Nogueira, J. Comput. Phys. **105** (1993), 406.
- [24] M. Steinhauser, Comput. Phys. Commun. **134** (2001), 335.
- [25] D.J. Broadhurst, Eur. Phys. J. **C8** (1999), 311.
- [26] O.V. Tarasov, Phys. Rev. **D54** (1996), 6479.
- [27] O.V. Tarasov, Nucl. Phys. **B502** (1997), 455.
- [28] R. Mertig & R. Scharf, Comput. Phys. Commun. **111** (1998), 265.
- [29] S.A. Larin & J.A.M. Vermaseren, Phys. Lett. **B303** (1993), 334.
- [30] S.É. Derkachov, N.A. Kivel, A.S. Stepanenko & A.N. Vasil'ev, hep-th/9302034.
- [31] A.N. Vasil'ev, S.É. Derkachov, N.A. Kivel & A.S. Stepanenko, Theor. Math. Phys. **94** (1993), 179.
- [32] A.N. Vasil'ev, & A.S. Stepanenko, Theor. Math. Phys. **97** (1993), 364.
- [33] J.A. Gracey, Phys. Lett. **B297** (1992), 293.
- [34] J.A. Gracey, Int. J. Mod. Phys. **A6** (1991), 395, 2755(E).
- [35] J.A. Gracey, Int. J. Mod. Phys. **A9** (1994), 567.
- [36] J.A. Gracey, Int. J. Mod. Phys. **A9** (1994), 727.
- [37] R. Dashen & Y. Frishman, Phys. Lett. **B46** (1973), 439.
- [38] R. Dashen & Y. Frishman, Phys. Rev. **D11** (1975), 2781.
- [39] J.A.M. Vermaseren, S.A. Larin & T. van Ritbergen, Phys. Lett. **B405** (1997), 327
- [40] T. van Ritbergen, J.A.M. Vermaseren & S.A. Larin, Phys. Lett. **B400** (1997), 379